

Nickel-coated polystyrene microsphere electrodes boost power output of silicon nanowire hydrovoltaic devices

Chenyang GU^{1,4†}, Xingshan JIANG^{1†}, Bingchang ZHANG^{1*}, Binbin ZHANG², Zhen LIU³,
Jia YU², Cheng ZHANG^{1*} & Xiaohong ZHANG^{2*}

¹ School of Optoelectronic Science and Engineering, Key Laboratory of Advanced Optical Manufacturing Technologies of Jiangsu Province, Key Laboratory of Modern Optical Technologies of Education Ministry of China, Soochow University, Suzhou 215006, China

² Institute of Functional Nano and Soft Materials (FUNSOM), Jiangsu Key Laboratory of Advanced Negative Carbon Technologies, Soochow University, Suzhou 215123, China

³ School of Materials Science and Engineering, Changzhou University, Changzhou 213164, China

⁴ Faculty of Engineering, Lund University, Lund 22100, Sweden

Received November 29, 2024; accepted March 6, 2025; published online May 14, 2025

Abstract The hydrovoltaic device (HD) based on silicon nanowires (SiNWs) is a promising green energy technology; however, efficient carrier collection remains a key challenge that limits the output performance of SiNW-based HDs. In this study, we propose using conductive microspheres as the top electrode to enhance carrier collection and improve the power output of SiNW HDs. Stacked nickel-coated polystyrene microspheres conformally contact the top surface of the SiNW array, facilitating efficient carrier collection from individual SiNWs and enabling effective parallel connection of multiple SiNW hydrovoltaic microunits. Optimal microsphere parameters, specifically a 10 μm diameter and 2.8 mg cm^{-2} deposition density, are identified, balancing the positive effects of charge collection with the negative impact of water microflow induced by microsphere deposition. After optimization, the open-circuit voltage of SiNW HDs increases by 21%, and the maximum output power density rises by 49%, from 0.67 V and 8.2 $\mu\text{W cm}^{-2}$ in HDs without the microsphere electrode to 0.81 V and 12.2 $\mu\text{W cm}^{-2}$ in HDs with the microsphere electrode. This work provides a simple yet effective solution to the carrier collection problem in SiNW HDs, offering a significant step forward in the development and application of high-performance SiNW HDs.

Keywords hydrovoltaic devices, silicon nanowires, conductive microspheres, carrier collection, microsphere electrodes

Citation: Gu C Y, Jiang X S, Zhang B C, et al. Nickel-coated polystyrene microsphere electrodes boost power output of silicon nanowire hydrovoltaic devices. *Sci China Tech Sci*, 2025, 68(6): 1620203, <https://doi.org/10.1007/s11431-024-2919-7>

1 Introduction

Water, as a green and renewable energy source, has been harnessed for centuries. Covering 71% of the Earth's surface, it serves as the planet's largest energy carrier [1]. Natural water bodies absorb approximately 35% of the solar energy incident on Earth, amounting to a staggering 60 petawatts (10^{15} W) annually [2]. If just 0.03% of this energy could be

captured, it would be sufficient to meet global energy demands [3]. However, traditional hydroelectric technologies are only capable of harnessing a fraction of the available hydraulic energy, leaving the majority as micromechanical energy distributed throughout the water [4,5].

In 1861, Quincke [6] first reported that water flowing through a narrow channel under a pressure gradient generates a voltage due to interactions between the water and solid surfaces, a phenomenon known as streaming potential. Recently, with advancements in nanotechnology, studies have revealed that the directed motion of water within na-

[†] These authors contributed equally to this work.

* Corresponding author (zhangbingchang@suda.edu.cn; zhangc@suda.edu.cn; xiaohong_zhang@suda.edu.cn)

nochannels induces the movement of charge carriers in the channel walls, generating an electric potential known as the hydrovoltaic effect [7–11]. This effect has been observed in a variety of materials, including carbon-based nanomaterials, semiconductor nanostructures, organic nanomaterials, and composites [10–14]. Among these, silicon nanowire (SiNW) arrays have demonstrated exceptional potential due to their highly ordered nanochannels [15–17]. In SiNW hydrovoltaic devices (HDs), each SiNW serves as a hydrovoltaic microunit, paralleled through common upper and bottom electrodes. This ordered parallel configuration significantly enhances the power output [18]. Moreover, SiNW arrays can be massively produced through metal-assisted chemical etching (MACE) and are compatible with silicon solar cells [19–22], making SiNW arrays highly promising for HDs. In recent years, considerable efforts have been made to improve the output performance of SiNW HDs, including optimizing SiNW structural parameters [23], surface modification [22], and interface passivation [24]. Despite these advancements, efficient carrier collection remains a significant challenge for SiNW HDs [18,25,26]. Given that water microflow drives the hydrovoltaic effect, the surface of the SiNW array must be open to allow water flow through the microchannels (Figure 1(a)). This requirement means that the electrode cannot fully cover the array, making it difficult to connect every individual nanowire tip. In other words, the potential benefit of the microunit parallelism in SiNW HDs has not been fully realized, thus limiting the overall power output.

Conductive microspheres, which offer excellent conductivity, stability, and cost-effectiveness, have found widespread use as electrodes in fields such as catalysis, biomedicine, and lithium-ion batteries [1,4,25]. Stacked microspheres can conform to uneven surfaces, and the pores between microspheres provide space for water microflow. These attributes make conductive microspheres a promising material for improving carrier collection in SiNW HDs (Figure 1(b)). In this study, nickel-coated polystyrene microspheres (Ni-coated PSMSs) were employed as the top electrode for SiNW HDs. The conductive microspheres formed conformal contact with the top surface of the SiNW

array, facilitating efficient carrier collection from individual SiNWs. This effective parallel connection of numerous SiNW hydrovoltaic microunits significantly boosted the power output of the SiNW HDs. Moreover, optimized parameters, including the diameter and deposition density of the Ni-coated PSMSs, were investigated. These parameters strike a balance between enhancing charge collection and mitigating the impact of water microflow disruption caused by the microsphere deposition. With optimal microsphere parameters of 10 μm in diameter and 2.8 mg cm^{-2} deposition density, the open-circuit voltage of the SiNW HDs increased by 21%, and the maximum output power density rose by 49%. Specifically, the open-circuit voltage increased from 0.67 V and the maximum output power density from 8.2 $\mu\text{W cm}^{-2}$ (without the microsphere electrode) to 0.81 V and 12.2 $\mu\text{W cm}^{-2}$ (with the microsphere electrode). This work presents a simple and effective strategy for enhancing the power output of SiNW HDs.

2 Experimental procedure

2.1 Fabrication and characterization of SiNWs

The fabrication of SiNWs commenced with n-type (100)-oriented silicon wafers, characterized by a thickness of 500 μm , single-side polishing, and resistivity ranging from 0.01 to 0.05 $\Omega\text{ cm}$. These wafers were precisely sectioned into 2 cm \times 2 cm specimens using a 350 nm, 20 W laser system (Hanhonglaser, TH-UVLMS5). Prior to nanowire formation, the silicon substrates underwent a rigorous cleaning protocol involving sequential ultrasonication in acetone, ethanol, and deionized water (each solvent 20 min), followed by nitrogen-assisted drying.

The nanowire fabrication employed the MACE technique [19–22], which involved two distinct etching stages. Initially, the substrates were treated with a seeding solution comprising 2.5 mmol L^{-1} AgNO_3 and 4.8 mol L^{-1} HF at 35°C for 60 s. Subsequently, the primary etching process was conducted using a solution containing 0.4 mol L^{-1} H_2O_2 and 4.8 mol L^{-1} HF at 35°C for 40 min. To ensure purity, the

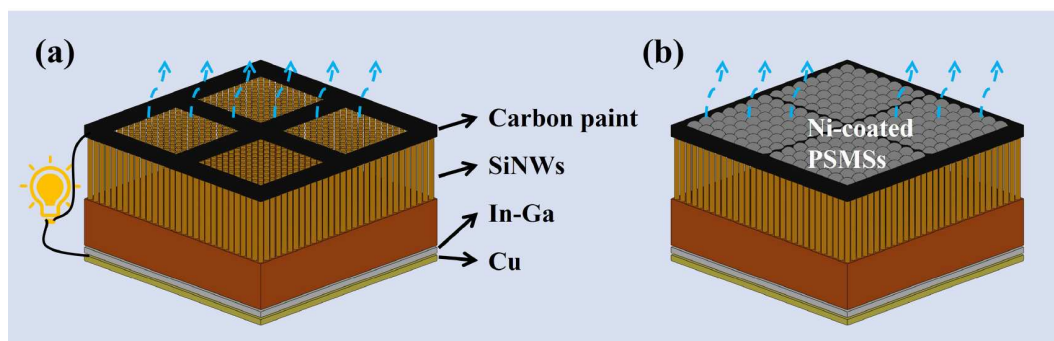


Figure 1 (Color online) Schematic diagram of the SiNW HD (a) without and (b) with the Ni-coated microsphere electrode.

resulting SiNWs were subjected to a 10-minute immersion in HNO_3 to remove any residual silver, followed by a 5-minute deionized water rinse and nitrogen drying. Structural characterization of the synthesized SiNWs was performed using a SU5000 scanning electron microscope to analyze surface morphology.

2.2 Fabrication of Ni-coated PS microspheres

Ni-coated PS microspheres were prepared by electroless nickel plating of PS microspheres (PSMSs) purchased from Jiangsu Zhichuan Technology Co., Ltd. (China). The microspheres were first sensitized by immersing them for 2 h in a solution containing $0.2 \text{ mol L}^{-1} \text{ SnCl}_2$ and $1.2 \text{ mol L}^{-1} \text{ HCl}$. This was followed by a 20-minute activation process at 50°C using a solution containing $2.8 \text{ mmol L}^{-1} \text{ PdCl}_2$. The final step involved electroless nickel plating at 55°C for 25 min using a plating bath composed of $0.4 \text{ mol L}^{-1} \text{ NiSO}_4 \cdot 6\text{H}_2\text{O}$, $0.9 \text{ mol L}^{-1} \text{ NaH}_2\text{PO}_2$, and $0.2 \text{ mol L}^{-1} \text{ Na}_3\text{C}_6\text{H}_5\text{O}_7 \cdot 2\text{H}_2\text{O}$. During the plating process, the stirring speed was maintained at 100 r min^{-1} .

2.3 Fabrication and characterization of SiNW HDs

To construct the basic SiNW HDs, the backside of the SiNWs was coated with an indium-gallium (In-Ga) alloy to establish contact with a copper substrate. On the front side, intersecting carbon electrodes were applied as the top elec-

trodes and connected to a copper wire. For SiNW HDs with a microsphere electrode, Ni-PS microsphere suspensions at varying concentrations were dropped onto the surface of the SiNWs in the basic HDs. The deposited Ni-PS microspheres acted as the conjoint top electrode, which was connected to the existing carbon electrodes. The electrical characteristics of the SiNW HDs were measured using an electrochemical analyzer (CHI630E).

3 Results and discussion

3.1 Fabrication and characterization of Ni-coated PSMSs

Nickel-coated polystyrene microspheres were selected as the top electrode for SiNW HDs due to their excellent size controllability, low cost, strong corrosion resistance, and commercial availability. The PSMSs were prepared by electroless nickel plating on commercially available PSMSs. PSMSs with diameters of 1, 5, and $10 \mu\text{m}$ were used. These samples exhibited good monodispersity in particle size (Figure S1 (Supporting Information)) and were characterized using scanning electron microscopy (SEM) (Figure 2(a)–(c)). Each sample displayed a uniform spherical morphology, which facilitates the formation of water circulation channels between the microspheres when accumulated. After the nickel coating, the color of the PSMSs changed from white to black (Figure 2(d) and (e) insets). Under optical microscopy,

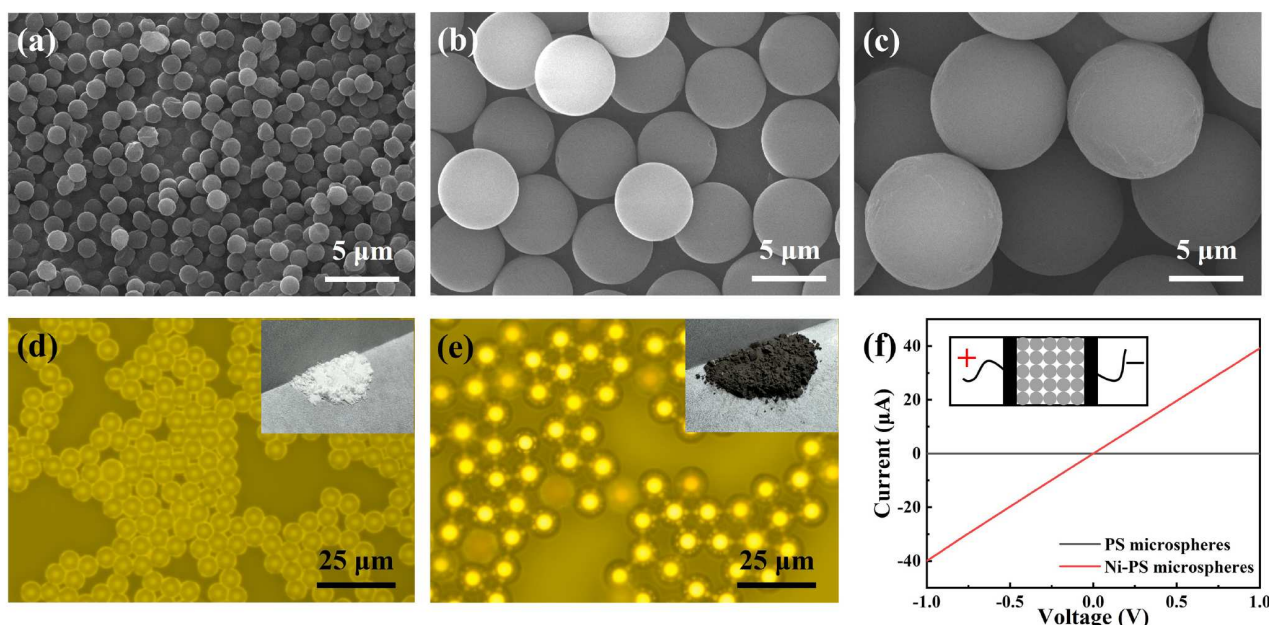


Figure 2 (Color online) Morphology and electrical properties of PSMSs before and after nickel coating. (a)–(c) SEM images of PSMSs with diameters of 1 μm (a), 5 μm (b), and 10 μm (c), showing uniform spherical morphology; (d) optical microscope image and photograph (inset) of uncoated PSMSs, exhibiting a matte white appearance; (e) optical microscope image and photograph (inset) of Ni-coated PSMSs, displaying a metallic luster and black coloration; (f) current-voltage (I - V) curves of PSMSs before and after nickel coating, demonstrating enhanced electrical conductivity after coating. The inset shows the setup for electrical measurement.

the Ni-coated PSMSs exhibited a metallic luster with strong reflection (Figure 2(e)), whereas the original PSMSs reflected light relatively weakly (Figure 2(d)), indicating successful deposition of the nickel layer on the surface of the microspheres.

The electrical conductivity of the samples was characterized to assess the suitability of the Ni-coated PSMSs as electrodes (Figure 2(f)). Both the uncoated and Ni-coated PSMSs were deposited between two carbon paste electrodes. The horizontal current-voltage curve of the PSMS sample indicates the non-conductivity of original PSMSs. In contrast, the Ni-coated PSMS sample shows good conductivity with a resistance of 25.3 k Ω . This suggests that Ni-coated PSMSs can be used as conductive electrodes with the capability of conformal contact with microscale rough surfaces. Furthermore, the contact between Ni-coated PSMSs and the used silicon wafer (n-type, heavily doped, 0.01–0.05 Ω cm) was tested (Figure S2). No typical Schottky barrier was observed; instead, the contact exhibited Ohmic behavior, confirming that the Ni-coated PSMSs are suitable for use as the conjoint top electrode to efficiently collect carriers from the SiNWs.

3.2 Optimization of Ni-coated PSMS electrodes in SiNW HDs

To fabricate SiNW HDs, aligned SiNW arrays were first prepared using the MACE method (Figure 3(a)). Indium-gallium (In-Ga) alloy was used to connect the SiNW arrays to copper substrates, serving as the bottom electrode. For SiNW HDs without the microsphere electrode, multiple carbon paint grids were employed as the top electrode (Figure 1(a)). In contrast, for SiNW HDs with the microsphere electrode, Ni-coated PSMSs were deposited as the conjoint top electrode in addition to the grid top electrode (Figure 1(b)). As shown in Figure 3(b), the Ni-coated PSMSs conformally contact the surface of the SiNW array, forming effective conductive paths. The inclusion of the microsphere conjoint electrode leads to a noticeable improvement in device performance. For instance, the open-circuit voltage increased from 0.67 to 0.81 V when 10 μ m Ni-coated PSMSs were deposited on the device surface at a density of 2.8 mg cm⁻² (Figure 3(c)).

To identify the optimal conditions for fabricating the microsphere electrode, the effects of the deposition density and diameter of the Ni-coated PSMSs on the open-circuit voltage of SiNW HDs were systematically investigated. The same base device was used for consistency, and the Ni-coated PSMSs with different parameters served as the variables, ensuring that any observed effects were due to the microsphere modifications rather than device variability. First, 10 μ m Ni-coated PSMSs with varying deposition densities were applied as the conjoint top electrode. As the deposition

density increased from 0 to 2.8 mg cm⁻², the open-circuit voltage of the SiNW HDs gradually increased (Figure 3(d)). When the density further increased from 2.8 to 3.5 mg cm⁻², the open-circuit voltage reached saturation. When 1 and 5 μ m Ni-coated PSMSs were used as the conjoint top electrodes, the open-circuit voltage of the SiNW HDs first increased and then decreased as the deposition density increased (Figure 3(e)). The optimum deposition density for both 1 and 5 μ m Ni-coated PSMSs was found to be 2.8 mg cm⁻². Moreover, it was observed that the open-circuit voltage of the SiNW HDs increased with the microsphere diameter when the deposition density was held constant. At the optimal deposition density of 2.8 mg cm⁻², the open-circuit voltages were 0.72, 0.74, and 0.78 V for HDs with 1, 5, and 10 μ m microsphere electrodes, respectively (Figure 3(e)). These results indicate that the performance improvement of SiNW HDs is closely related to both the deposition density and diameter of the Ni-coated PSMSs. A suitable deposition density and larger microsphere diameter both contribute to enhanced device performance.

3.3 Mechanisms of performance optimization in SiNW HDs with microsphere electrodes

The hydrovoltaic mechanism of SiNW HDs can be explained as follows. At the solid-liquid interface, an electron double layer forms due to the electrostatic attraction between opposite charges in the solid and liquid phases. The surface of n-type silicon is negatively charged, creating a diffusion layer rich in cations on the solution side, within a length known as the Debye length. In HDs based on SiNW arrays, numerous nanopores exist between the SiNWs, with pore sizes on the order of hundreds of nanometers, which are smaller than the Debye length (\sim 1 μ m) at the solid-liquid interface [15]. This results in overlapping diffusion layers from the solid/liquid interfaces of different sidewalls within the nanopores. Consequently, the nanopores become enriched with cations and exhibit high selectivity for cations. As water evaporates, cyclic water flow forms within the system. The ions in the water move along with the flow, filling the nanopores (Figure 4(a)). Due to the cation selectivity of the nanopores, cations such as H₃O⁺ accumulate at the bottom of the pores, creating a concentration gradient of H₃O⁺, which in turn generates a potential difference along the vertical direction (Figure 4(b)). This results in an electron concentration gradient and a potential difference in the vertical direction within the SiNWs, due to Coulomb interactions between electrons in the SiNWs and H₃O⁺ in the water. This potential difference generates electrical power, which can be extracted through electrodes positioned at the top and bottom of the SiNW array.

Based on this understanding, it is essential to establishing proper contact with the top of each SiNW through a suitable

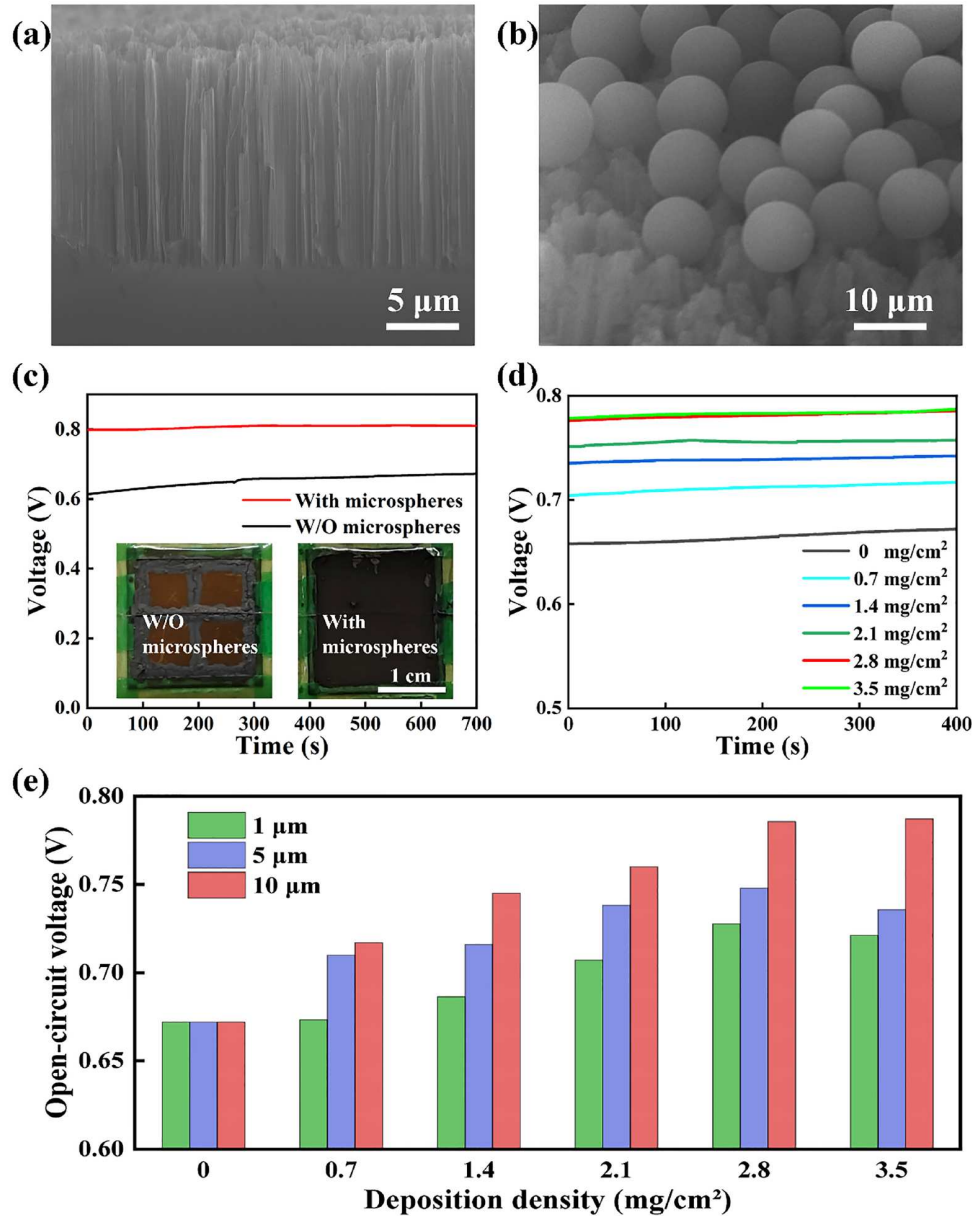


Figure 3 (Color online) Characterization of SiNW HDs. (a) Cross-section SEM image of a SiNW array; (b) 45° oblique-view SEM image of 10 μm Ni-coated PSMSs depositing on the surface of the SiNW array; (c) open-circuit voltages of SiNW HDs with/without the Ni-coated PSMS electrode. Insets are photographs of SiNW HDs with/without the Ni-coated PSMS electrode; (d) open-circuit voltages of SiNW HDs with different deposition densities of 10 μm Ni-coated PSMSs; (e) relationship between open-circuit voltages of SiNW HDs and deposition densities of Ni-coated PSMSs with diameters of 1, 5, and 10 μm, respectively.

electrode, such as Ni-coated PSMSs. SEM characterization reveals that the Ni-coated PSMSs conform well to the uneven surface of the SiNW array, effectively contacting the SiNW tips below (Figure 4(c)). The adjacent microspheres form electrically conductive paths that span the boundary between the carbon paint and SiNWs, connecting to the carbon paint grids (Figure 4(d)). In this configuration, charge carriers accumulated at the SiNW tips are collected by the Ni-coated PSMSs and transported to the carbon grids (Figure 4(e)). As a result, more SiNW hydrovoltaic microunits are

effectively paralleled for power output by depositing microsphere electrodes, compared to SiNW HDs without microsphere electrodes. Consequently, SiNW HDs with microsphere conjoint electrodes exhibit superior hydrovoltaic performance.

The impact of the deposition density and diameter of the Ni-coated PSMSs on HD performance can be understood by considering both carrier collection and water microflow. When the deposition density is low, carrier collection and conduction become the limiting factors. As the deposition

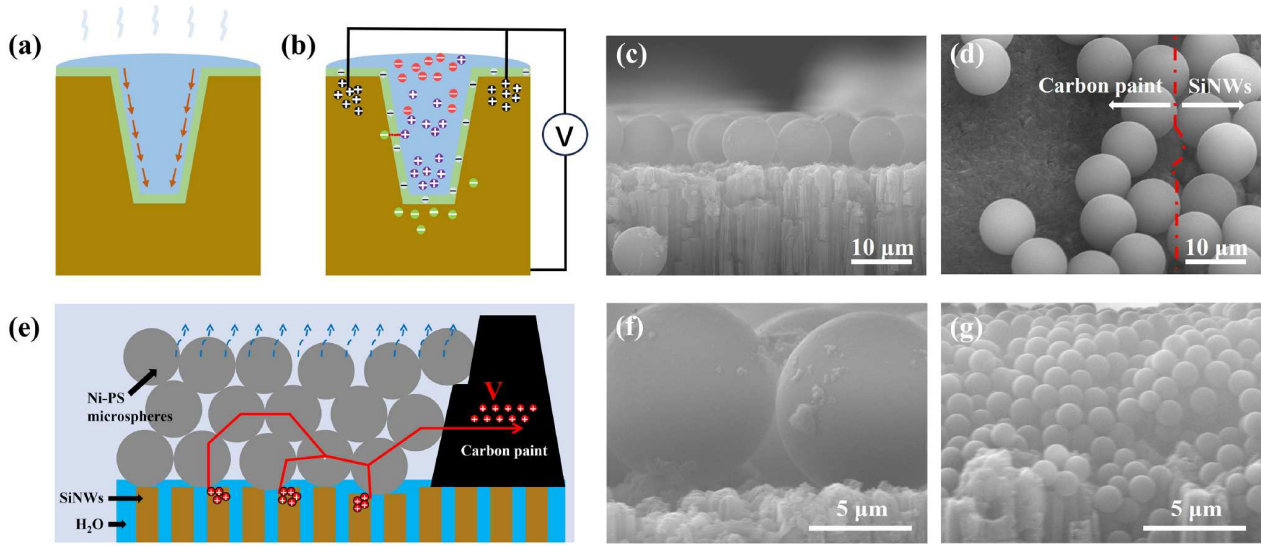


Figure 4 (Color online) Mechanism of performance enhancement in SiNW HDs with Ni-coated PSMS electrodes. (a) Schematic diagram of the internal circulation during the evaporation of droplets on the surface of SiNWs; (b) schematic diagram of the SiNWs HDs' power generation mechanism; (c) cross-section SEM image of 10 μm Ni-coated PSMSs depositing on the SiNW array; (d) 45° oblique-view SEM image of the distribution of 10 μm Ni-coated PSMSs at the interface between SiNWs and carbon paint; (e) schematic diagram of charge carrier collection and transport in SiNW HDs with the Ni-coated PSMS electrode; cross-sectional SEM images comparing the contact morphology of 10 μm (f) and 1 μm (g) Ni-coated PSMSs with SiNW tips, revealing the effect of microsphere size on water microflow pathways.

density increases, conductive paths are improved, and more SiNWs are interconnected, resulting in enhanced HD performance. However, once the deposition density reaches a certain threshold, water microflow becomes the limiting factor. Water microflow is the energy source for the hydrovoltaic effect [4,27,28]. Excessive deposition of Ni-coated PSMSs obstructs the movement of water microflow towards the SiNW array, leading to a decline in performance. Therefore, optimal HD performance depends on a moderate deposition density of Ni-coated PSMSs, which ensures effective conductive paths while minimally affecting water microflow. Additionally, SEM images of the SiNW-microsphere interfaces at the same magnification reveal that smaller Ni-coated PSMSs are packed more densely at the same deposition density (Figure 4(f) and (g)). This densely packed structure inhibits water microflow. This observation explains the experimental result that SiNW HDs with larger Ni-coated PSMSs for the conjoint top electrode exhibit higher open-circuit voltage at the same deposition density.

3.4 Comparative output performance of SiNW HDs with and without microsphere electrodes

Finally, the output performance of SiNW HDs with and without the microsphere electrode was comparatively evaluated. For the device with the microsphere electrode, 10 μm Ni-coated PSMSs with a deposition density of 2.8 mg cm^{-2} were used as the conjoint top electrode. The devices were tested under different external load resistances. In both cases,

the output voltage increased with the increase in load resistance (Figure 5(a)), while the output current density decreased as the load resistance increased (Figure 5(b)). The output power density exhibited a characteristic behavior, initially increasing and then decreasing with the increase in load resistance (Figure 5(c)). These results follow the typical behavior expected when a power source is connected to a load, consistent with Kirchhoff's laws and load characteristic theory [29]. Notably, the output voltage, current density, and power density of the HD with microsphere electrodes were consistently higher than those of the HD without microsphere electrodes for a given load resistance. At the optimal load resistance of 10 k Ω , the output power density increased by 49%, from $8.2 \mu\text{W cm}^{-2}$ in the HD without the microsphere electrode to $12.2 \mu\text{W cm}^{-2}$ in the HD with the microsphere electrode. These results demonstrate that the output performance of SiNW HDs can be significantly enhanced by incorporating Ni-coated PSMSs as the conjoint top electrode.

For practical applications, multiple SiNW HDs can be connected in series to provide a sufficient output voltage to match external loads. As shown in Figure 5(d), the output voltage is directly proportional to the number of devices connected in series, and the advantage of SiNW HDs with microsphere electrodes becomes even more pronounced in a series configuration. The output voltage of four HDs without microsphere electrodes is 2 V, while the output voltage of four HDs with microsphere electrodes reaches 2.6 V. To demonstrate the application potential of these devices, an

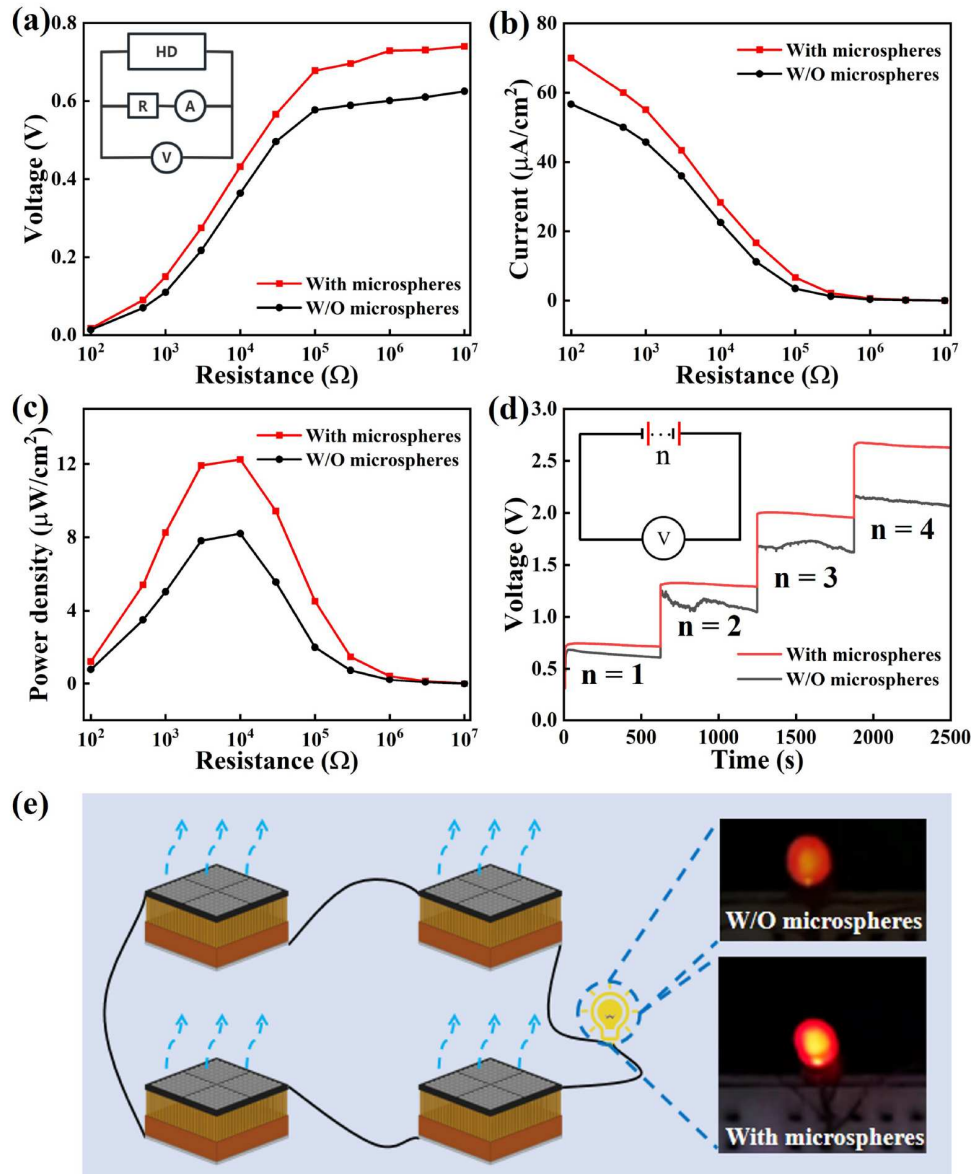


Figure 5 (Color online) Comparative performance evaluation and practical application of SiNW HDs. (a) Output voltages, (b) output current densities, and (c) output power densities of SiNW HDs with/without the Ni-coated PSMS electrode when they were connected to different external loads. Inset in (a) is the schematic diagram of the test setup; (d) open-circuit voltage as a function of the number of SiNW HDs connected in series, showing improved scalability with Ni-coated PSMS electrodes; (e) photograph of a commercial LED powered by four series-connected SiNW HDs, with enhanced brightness observed in devices utilizing microsphere electrodes.

LED with a threshold voltage of 2 V was used as a load. Four SiNW HDs, both with and without microsphere electrodes, were connected in series as power sources. As shown in Figure 5(e), the LED is visibly brighter when connected to the SiNW HDs with microsphere electrodes, further confirming the superior performance of the SiNW HDs with Ni-coated PSMS electrodes in practical applications. Lastly, it is important to note that the microspheres may become unstable under extreme conditions, such as strong water flow. This issue can be addressed by overlaying the microspheres with a conductive fabric (e.g., graphite/PEDOT:PSS/cellu-

lose fabrics) or using an adhesive (e.g., PVA) to secure the microspheres in place [25].

4 Conclusion

In summary, this work introduces a strategy to enhance the power output of SiNW HDs by employing Ni-coated PSMSs as the conjoint top electrodes. The Ni-coated PSMSs were fabricated through electroless nickel plating on PSMSs and were designed to conformally contact the top surface of the

SiNW array, thereby facilitating effective carrier collection from individual SiNWs. The optimal deposition conditions for the microspheres were determined by investigating the effects of both the deposition density and the diameter of the Ni-coated PSMSs on the open-circuit voltage of the SiNW HDs. The results revealed that the best performance enhancement occurred when the Ni-coated PSMSs were deposited with a density of 2.8 mg cm^{-2} and a diameter of $10 \text{ }\mu\text{m}$. These optimal conditions strike a balance between the positive effect of improved charge collection and the negative impact on water microflow caused by the microsphere deposition. Under these conditions, the maximum output power density increased by 49%, from $8.2 \text{ }\mu\text{W cm}^{-2}$ in the HD without the microsphere electrode to $12.2 \text{ }\mu\text{W cm}^{-2}$ in the HD with the microsphere electrode. The superior performance of the SiNW HDs with microsphere electrodes was further validated by their application in powering an LED. This approach, utilizing conductive microspheres as the top electrode, offers a promising method for improving the power output of SiNW HDs, advancing the development and practical application of high-performance SiNW HDs. However, despite the optimization of device performance in this study, the long-term robustness of SiNW HDs remains a critical concern, as device performance tends to degrade over the first 24 hours of operation due to the formation of a native oxide layer on the surface of the SiNWs [23]. Future work may focus on enhancing the robustness of the devices through surface passivation techniques.

Acknowledgements This work was supported by the Key Project of Jiangsu Provincial Basic Research Plan (Grant No. BK20243031), the Major International (Regional) Joint Research Project of the National Natural Science Foundation of China (Grant No. 51920105005), the Foundation for Innovation Research Groups of the National Natural Science Foundation of China (Grant No. 51821002), the National Natural Science Foundation of China (Grant No. 62004134), the Open Project of Key Lab of Advanced Optical Manufacturing Technologies of Jiangsu Province (Grant Nos. ZZ2308, ZZ2112), the Suzhou Key Laboratory of Functional Nano & Soft Materials, the Collaborative Innovation Center of Suzhou Nano Science and Technology, the Suzhou Science and Technology Plan Projects (Grant No. SYG202124), the Natural Science Foundation of the Jiangsu Higher Education Institutions of China (Grant No. 20KJA510003), the Qinglan Project of Jiangsu Province of China, the Priority Academic Program Development of Jiangsu Higher Education Institutions (PAPD), the 111 Project, and the Joint International Research Laboratory of Carbon-Based Functional Materials and Devices.

Supporting Information The supporting information is available online at tech.scichina.com and link.springer.com. The supporting materials are published as submitted, without typesetting or editing. The responsibility for scientific accuracy and content remains entirely with the authors.

References

- Hou Y, Dong X, Li D, et al. Self-powered underwater force sensor based on a t-shaped triboelectric nanogenerator for simultaneous detection of normal and tangential forces. *Adv Funct Mater*, 2023, 33: 2305719

- Yin J, Zhou J, Fang S, et al. Hydrovoltaic energy on the way. *Joule*, 2020, 4: 1852–1855
- Hu T, Zhang K, Deng W, et al. Hydrovoltaic effects from mechanical-electric coupling at the water-solid interface. *ACS Nano*, 2024, 18: 23912–23940
- Li L, Wang X, Deng W, et al. Hydrovoltaic energy from water droplets: Device configurations, mechanisms, and applications. *Droplet*, 2023, 2: e77
- Wang X, Lin F, Wang X, et al. Hydrovoltaic technology: From mechanism to applications. *Chem Soc Rev*, 2022, 51: 4902–4927
- Quincke G V. Ueber die Fortführung materieller Theilchen durch strömende Elektrizität. *Annalen der Physik*, 1861, 189: 513–598
- Liu C, Ye C, Wu Y, et al. Atomic-scale engineering of cation vacancies in two-dimensional unilamellar metal oxide nanosheets for electricity generation from water evaporation. *Nano Energy*, 2023, 110: 108348
- Liu Z, Wang Q, Chen T, et al. Energy harvesting from carbon-based rope driven by capillary flow. *J Power Sources*, 2024, 618: 235193
- Liu Y, Yu F, Jiang Y, et al. High performance hydrovoltaic devices based on asymmetrical electrode design. *J Power Sources*, 2024, 613: 234874
- Yun Y J, Yoon O J, Son D I, et al. Metal/bacteria cellulose nanofiber bilayer membranes for high-performance hydrovoltaic electric power generation. *Nano Energy*, 2023, 118: 108934
- Liu J, Huang L, He W, et al. Moisture-enabled hydrovoltaic power generation with milk protein nanofibrils. *Nano Energy*, 2022, 102: 107709
- Zhang S Y, Fang S M, Li L X, et al. Geometry effect on water-evaporation-induced voltage in porous carbon black film. *Sci China Tech Sci*, 2021, 64: 629–634
- Zheng C, Chu W, Fang S, et al. Materials for evaporation-driven hydrovoltaic technology. *Interdiscip Mater*, 2022, 1: 449–470
- Xue G, Xu Y, Ding T, et al. Water-evaporation-induced electricity with nanostructured carbon materials. *Nat Nanotech*, 2017, 12: 317–321
- Qin Y, Wang Y, Sun X, et al. Constant electricity generation in nanostructured silicon by evaporation-driven water flow. *Angew Chem Int Ed*, 2020, 59: 10619–10625
- Song X, Zhang T, Wu L, et al. Highly stretchable high-performance silicon nanowire field effect transistors integrated on elastomer substrates. *Adv Sci*, 2022, 9: 2105623
- Sahafi P, Rose W, Jordan A, et al. Ultralow dissipation patterned silicon nanowire arrays for scanning probe microscopy. *Nano Lett*, 2020, 20: 218–223
- Song Y, Song Z, Jiang C, et al. Ferroelectric layer-assisted asymmetric heterojunction boosts power output in silicon hydrovoltaic device. *Adv Energy Mater*, 2023, 13: 2302765
- Chen H, Shi Y, Qin J, et al. Array density effect on the optical and photoelectric properties of silicon nanowire arrays via Ag-assisted chemical etching. *Nanotechnology*, 2023, 34: 405703
- Farhadi A, Bartschmid T, Bourret G R. Dewetting-assisted patterning: A lithography-free route to synthesize black and colored silicon. *ACS Appl Mater Interfaces*, 2023, 15: 44087–44096
- Huo C, Wang J, Fu H, et al. Metal-assisted chemical etching of silicon in oxidizing hf solutions: Origin, mechanism, development, and black silicon solar cell application. *Adv Funct Mater*, 2020, 30: 2005744
- Sheng G, Shi Y, Zhang B, et al. Surface modification of silicon nanowires with siloxane molecules for high-performance hydrovoltaic devices. *ACS Appl Mater Interfaces*, 2024, 16: 8024–8031
- Zhang B, Zhang B, Sheng G, et al. Modulating the density of silicon nanowire arrays for high-performance hydrovoltaic devices. *Nanotechnology*, 2024, 35: 185401
- Shao B, Xing C, Song Y, et al. Boosting electrical output of nanostructured silicon hydrovoltaic device via cobalt oxide enabled electrode surface contact. *Nano Energy*, 2023, 106: 108081
- Shao B, Song Z, Chen X, et al. Bioinspired hierarchical nanofabric

- electrode for silicon hydrovoltaic device with record power output. *ACS Nano*, 2021, 15: 7472–7481
- 26 Song Z, Ge C, Song Y, et al. Synergistic solar-driven freshwater generation and electricity output empowered by wafer-scale nanostructured silicon. *Small*, 2023, 19: 2205265
- 27 Ren G, Ye J, Hu Q, et al. Growth of electroautotrophic microorganisms using hydrovoltaic energy through natural water evaporation. *Nat Commun*, 2024, 15: 4992
- 28 Cai H, Guo Y, Guo W. Synergistic effect of substrate and ion-containing water in graphene based hydrovoltaic generators. *Nano Energy*, 2021, 84: 105939
- 29 Lan C, Liao Y, Hu G. A unified equivalent circuit and impedance analysis method for galloping piezoelectric energy harvesters. *Mech Syst Signal Process*, 2022, 165: 108339